Droplet behaviour in a Ranque-Hilsch vortex tube

2011 J. Phys.: Conf. Ser. 318 052013

(http://iopscience.iop.org/1742-6596/318/5/052013)

Journal of Physics: Conference Series **318** (2011) 052013 doi:10.1088/1742-6596/318/5/052013

Droplet behaviour in a Ranque-Hilsch vortex tube

R Liew[1], W R Michałek[2], J C H Zeegers[1] and J G M Kuerten[2,3]

[1] Department of Applied Physics, Eindhoven University of Technology, P.O. Box 513, 5600 MB Eindhoven, The Netherlands

[2] Department of Mechanical Engineering, Eindhoven University of Technology, P.O. Box 513, 5600 MB Eindhoven, The Netherlands

[3] Faculty EEMCS, University of Twente, P.O. Box 217, 7500 AE Enschede, The Netherlands

E-mail: r.liew@tue.nl

Abstract. The vortex tube is an apparatus by which compressed gas is separated into cold and warm streams. Although the apparatus is mostly used for cooling, the possibility to use the vortex tube as a device for removing non-desired condensable components from gas mixtures is investigated. To give first insight on how droplets behave in the vortex tube, a MATLAB model is written. The model tracks Lagrangian droplets in time and space according to the forces acting on the droplets. Phase interactions, i.e. evaporation or condensation, are modeled according to the kinetic approach for phase interactions. Liquid (water) concentrations are shown for two cases where the humidity at the inlet of the vortex tube is varied from 0% to 50%. It is clearly observed from the results that the concentration of liquid increases with increasing humidity. The higher this concentration is, the higher the probability that droplets collide with each other and form larger droplets which are swirled towards the wall to form an easy-to-separate liquid film.

1. Introduction

A vortex tube is an apparatus by which compressed gas is separated into cold and warm streams. The temperature separation effect was first discovered by Ranque (1933) and improved by Hilsch (1947).

In the vortex tube, pressurized gas is tangentially expanded to create a high swirling motion in the tube which is connected to the gas inlets (figure 1). The flow of gas is split in two parts. One part of the gas leaves the system through the diaphragm near the inlet and has a lower temperature than at the inlet. The remaining gas leaves the system at the other side of the tube with a higher temperature. The ratio of the two flow rates, as well as the temperature difference, is controlled by a valve. Simplicity and no moving parts have made the vortex tube popular for applications where compressed air is at disposal to generate cooling.

The unique combination of compressible flow, turbulence and local temperature decrease makes the vortex tube of potential interest as a device for removing non-desired condensable components from gas mixtures.

A MATLAB model is developed which simulates droplet behaviour in the vortex tube to estimate the droplet motion to determine where the liquid concentration. The results may be used for redesigning the vortex tube towards a separation device.

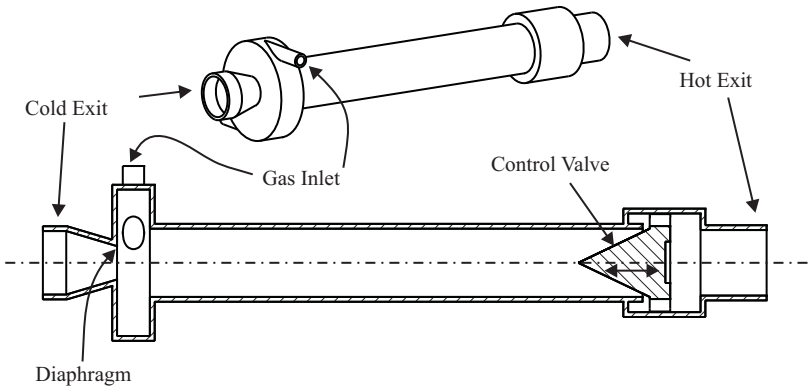

Figure 1: Schematic drawing of the Ranque-Hilsch Vortex Tube

2. Modeling of droplet behaviour in the vortex tube

2.1. Computational domain and flow conditions

In order to model droplet behaviour, a $2D$ axisymmetric domain is used which is based on an existing vortex tube that has already been used for velocity, temperature, pressure and turbulence measurements in previous research Gao (2005). The diameter of the vortex tube is 40 mm and the length $L = 2.586$ m. Z is the axial coordinate and r is the radial coordinate as shown in figure 2. The flow conditions of the continuous phase (nitrogen gas) in the vortex

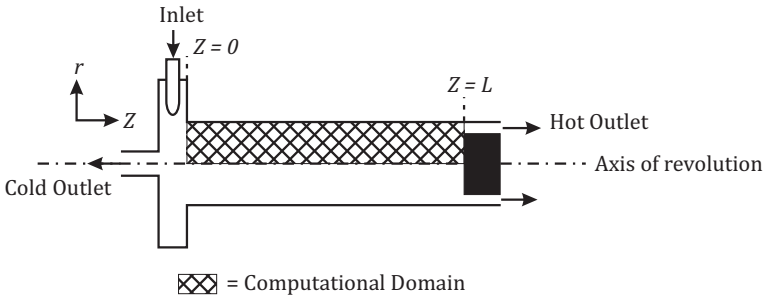

Figure 2: Schematic vortex tube where the hashed area is the computational domain

tube are taken from measurements obtained by (Gao, 2005) and are simplified and implemented in the model. The three-dimensional velocity is plotted in figure 3. Figure 3a gives the radial velocity component U_r near the inlet of the vortex tube as a function of the radius and axial coordinate. The figure shows that the radial velocity is decayed to zero after one vortex tube diameter. The swirl velocity U_θ is shown in figure 3b for $Z = 0$ and $Z = L/2$. Because of viscous decay of the vortex, the maximum swirl velocity decreases with Z/L. The diaphragm (figure 1) enables part of the gas to leave the vortex tube in negative Z direction. This causes negative axial velocity U_z in the core region and positive axial velocity near the walls of the vortex tube. The axial velocity as a function of r and Z/L is shown in figure 3c.

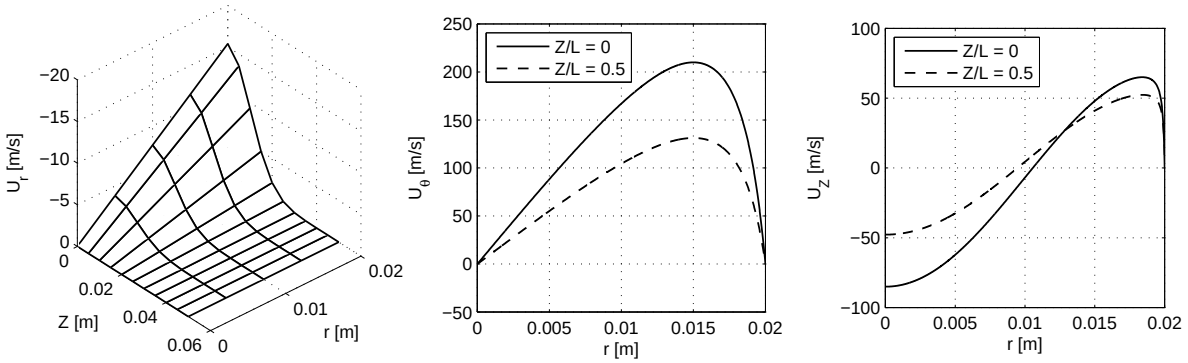

(a) (b) (c)

Figure 3: Velocity components as function of the vortex tube radius and length. (a) radial velocity component, (b) swirl velocity at $Z/L = 0$ and $Z/L = 0.5$ and (c) axial velocity at $Z/L = 0$ and $Z/L = 0.5$

Because of the high swirl velocity, the static pressure increases from the axis towards the wall, shown in figure 4a. The static temperature distribution was measured by Gao (2005) by means of a thermocouple and a cylindrical type pitot tube. The simplified temperature distribution used in the model is shown in figure 4b. Both the static pressure and static temperature are important for the phase interaction model, discussed in section 3.

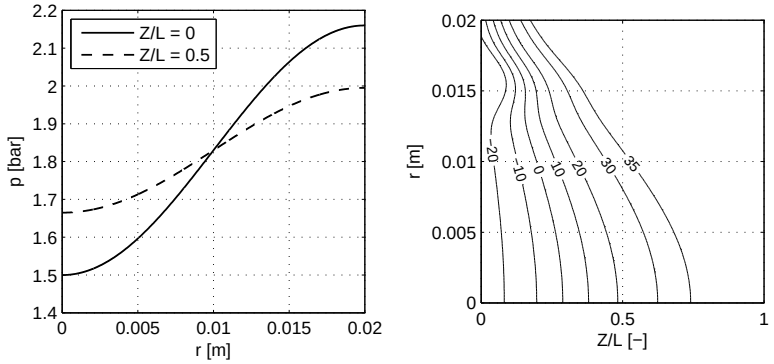

(a) (b)

Figure 4: Static pressure distribution (a) and static temperature distribution (b) used in the model (Gao, 2005).

2.2. Droplet properties

In this research, water droplets are used as dispersed phase. The droplets are assumed to be spherical and are considered as Lagrangian particles which do not disturb the flow. The forces acting on the droplets which are taken into account are the viscous friction of the fluid upon the droplet and the centrifugal force due to the swirl. Other forces are neglected because the density of the droplets is much higher than that of the gas. The equation of motion for droplets

reads

$$\frac{d\mathbf{v}}{dt} = \frac{\mathbf{u}-\mathbf{v}}{\tau_d}\left(1+0.15Re_d^{0.687}\right)+\mathbf{F} \tag{1}$$

where $\mathbf{v}$ is the velocity of a droplet with diameter d, $\mathbf{u}$ is the fluid velocity at the droplet position, τ_d is the droplet relaxation time given by

$$\tau_d = \frac{\rho_d d^2}{18\rho_f \nu} \tag{2}$$

and ρ_f is the fluid density and ν is the kinematic viscosity of the fluid. The Reynolds number is defined as

$$Re_d = \frac{|\mathbf{u}-\mathbf{v}|d}{\nu} \tag{3}$$

The assumption is made that the centrifugal force acts only in radial direction. Therefore, the force vector reads

$$\mathbf{F} = \begin{pmatrix} F_c \\ 0 \\ 0 \end{pmatrix} \tag{4}$$

with $F_c = m_d U_\theta^2/r$ the centrifugal force and m_d the mass of the droplet.

The mass fraction of water in the nitrogen gas due to droplet seeding is on the order of 10^{-3}. The droplet concentration, the added mass of water to the nitrogen and the possibility of droplet collisions is therefore neglected. Effects of turbulence on the droplet behaviour is neglected.

3. The influence of humidity on droplet behaviour

The nitrogen gas used in the experiments does not contain vapour. Because of the non-equilibrium in partial pressures, the droplets evaporate when they are introduced locally in the vortex tube. This is not desirable, because the droplets need to be separated from the gas. Humidifying the nitrogen before the droplets are added is used to partially overcome this problem. An additional effect caused by humidifying the nitrogen is that droplets in low temperature regions grow due to condensation. Both evaporation and condensation affect the behaviour of droplets and liquid concentration because of the change in centrifugal force. This all is implemented in the model to better understand the droplet behaviour.

The change of mass of a droplet m_d in time is given by

$$\frac{dm_d}{dt} = -2\pi\rho_v D_g d \ln(1+B_M) \tag{5}$$

(Sazhin, 2005; Sazhin *et al.*, 2005; Spalding, 1979) where ρ_v is the density of vapour, d the droplet diameter, D_g is the binary diffusion coefficient for water vapour in nitrogen gas (Bird *et al.*, 2007, p. 526) and $B_M = (Y_{fs} - Y_{f\infty})/(1-Y_{fs})$ the Spalding mass number (Spalding, 1979, p. 61). This model assumes that a single droplet is present in an infinite space with a defined humidity background of the ambient gas. The Spalding mass number gives the balance between the mass fraction of water vapour surrounding the droplet Y_{fs}, and in the ambient gas $Y_{f\infty}$. The mass fractions are calculated according to

$$Y_{f\infty} = \left[1+\left(\frac{p}{p_{part}}-1\right)\frac{M_{N_2}}{M_{H_2O}}\right] \tag{6}$$

where p is the ambient pressure, p_{part} the partial pressure of water vapour, M_{N_2} and M_{H_2O} are the molar masses of nitrogen and water respectively. These properties (except the ambient

pressure) are evaluated near the droplet surface (subscript s) or in the ambient gas (subscript ∞) to find both mass fractions. The partial pressure of vapour in the continuous phase depends on the relative humidity $RH = \frac{p_{part}}{p_{sat}}$. Near the surface of the droplet it is assumed that $RH = 1$ which implies that $p_{part} = p_{sat}(T_d)$, the saturation pressure evaluated at the droplet temperature T_d. In the ambient gas, the partial vapour pressure varies according to $p_{part} = RHp_{sat}(T_a)$, evaluated at the nitrogen temperature T_a. The local humidity is found from $RH = p\theta/p_{sat}$ assuming a constant non-dimensional molecular concentration of vapour molecules in the nitrogen gas which is defined at the inlet: $\theta = p_{sat}(T_{in})RH_{in}/p_{in}$. This implies that the partial vapour pressure in the ambient gas is taken to be constant. In real life however, condensation or evaporation may change the partial vapour pressure significantly. The temperature change in the nitrogen gas due to condensation or evaporation is neglected here assuming that the heat capacity of the gas is much higher than the heat absorbed or released due to evaporation or condensation. The change in droplet temperature T_d in time is then given by

$$\frac{dT_d}{dt} = \frac{Q_h + Q_l}{m_p c_p} \tag{7}$$

where $Q_h = 2\pi dk(T_a - T_p)$ is the convective heat transfer from the gas to the droplet assuming that the Nusselt number $Nu = hd/k \approx 2$ for small droplets (Janna, 2000). $Q_l = \frac{dm_d}{dt} h_{fg}$ is the heat released due to phase changes, k is the thermal conductivity of the gas mixture, c_p the heat capacity of water, h the convective heat transfer coefficient and h_{fg} the latent heat of evaporation.

4. Results

The radial droplet position as a function of the dimensionless axial coordinate Z/L is computed for three initial droplet positions ($r_0 = 15, 17$ and 19 mm). The initial droplet size is taken to be $d_{init} = 0.5\mu$m. The result for $RH = 0$ is shown in figure 5 where the different line styles correspond to the three different initial droplet positions. Due to negative radial flow near

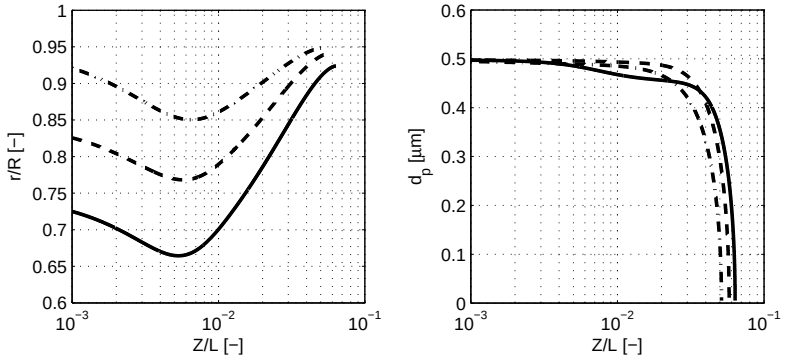

(a) (b)

Figure 5: Result for a 0.5μm initial diameter droplet and $RH_{in} = 0$. (a) Dimensionless droplet position (droplets move from left to right) and (b) droplet diameter. Both are plotted as functions of the dimensionless axial coordinate. The different lines denote droplets released from different radial positions.

the inlet, the droplets move towards the axis of the vortex tube. When the centrifugal force

overcomes the radial drag force, the droplets move towards the wall. This is clearly observed from figure 5a. Because the vapour pressure in the gas is zero ($RH_{in} = 0$), the droplets evaporate.

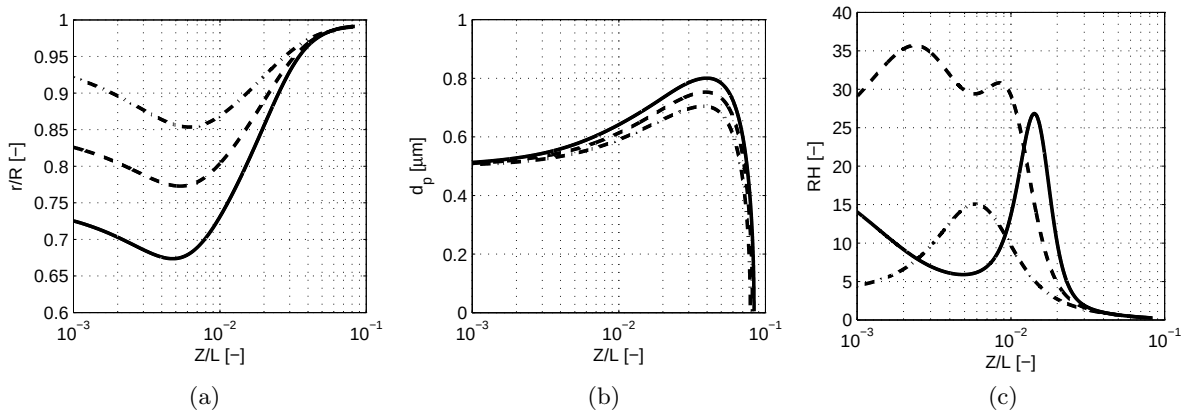

(a) (b) (c)

Figure 6: Result for a 0.5μm initial diameter droplet and $RH_{in} = 0.5$. (a) Dimensionless droplet position (droplets move from left to right), (b) droplet diameter and (c) relative humidity at droplet position. All are plotted as functions of the dimensionless axial coordinate. The different lines denote droplets released from different radial positions.

Figure 5b shows the changing size of droplets as a function of Z/L. The droplets are evaporated at $Z/L > 0.063$ ($Z = 16$ cm).

Droplets evaporate more slow or even grow because of condensation if there is already vapour present in the ambient gas ($RH_{in} > 0$). Figure 6 shows the droplet behaviour when the gas is pre-humidified. The relative humidity at the inlet is $RH_{in} = 0.5$, the local humidity however, increases in some regions where the temperature is lower. In the warm regions of the vortex tube the humidity drops again. The local humidity at the droplet position is shown in figure 6c. It shows that the temperature is that low, that the vapour present in the nitrogen gas is supersaturated. In this region the vapour condenses onto the droplets, which therefore grow as shown in figure 6b. The increased mass of the droplets causes a larger centrifugal force accelerating the droplets faster towards the wall (comparing figure 5a and 6a).

The same analysis is made for a small droplet of $d_{init} = 0.1\mu$m. Figure 7 shows that a small droplet evaporates quickly (figure 7b) if $RH_{in} = 0$. The centrifugal force is at all times less than the radial drag force. Because of this, droplets move towards the axis while evaporating, as shown in figure 7a and 7b. In this case droplets cannot be separated, because they evaporate before colliding with the wall.

However, pre-humidifying the nitrogen leads to condensation of vapour onto the droplets which therefore grow. Figure 8 shows that the lifetime (the time until the droplet vanishes) is increased and that droplets travel a longer distance before they vanish. This happens very close to the wall and it is expected that turbulence enables the droplets to hit the wall and form a liquid film which is easy to extract from the gas. Because of the growth of the droplets in the region where the vapour is supersaturated ($RH > 1$, figure 8c), the centrifugal force becomes larger and overcomes the radial drag force (figure 8a). From figure 8b it is seen, that the droplet size is increased by a factor of 7.5 due to condensation. This is much more than the previous result for a $d_{init} = 0.5\mu$m droplet, where the increase in size is only a factor of 1.6 (figure 6b). The difference in increase in droplet mass is even more distinct: For the $d_{init} = 0.1\mu$m droplet, the increase in mass is a factor of 420 while for the $d_{init} = 0.5\mu$m case, this is 'only' a factor of 4.

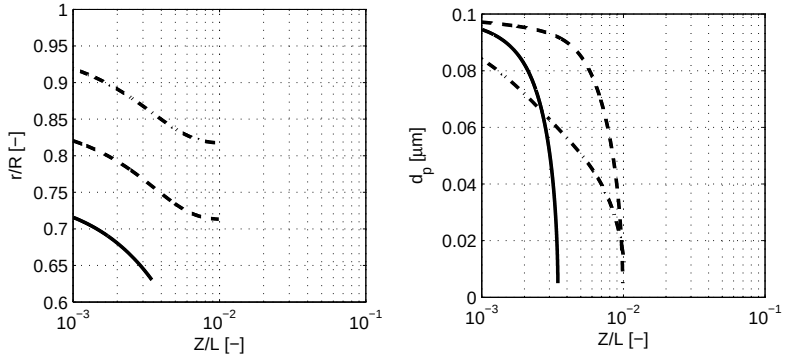

(a) (b)

Figure 7: Result for a 0.1μm initial diameter droplet and $RH_{in} = 0$. (a) Dimensionless droplet position (droplets move from left to right) and (b) droplet diameter. Both are plotted as functions of the dimensionless axial coordinate. The different lines denote droplets released from different radial positions.

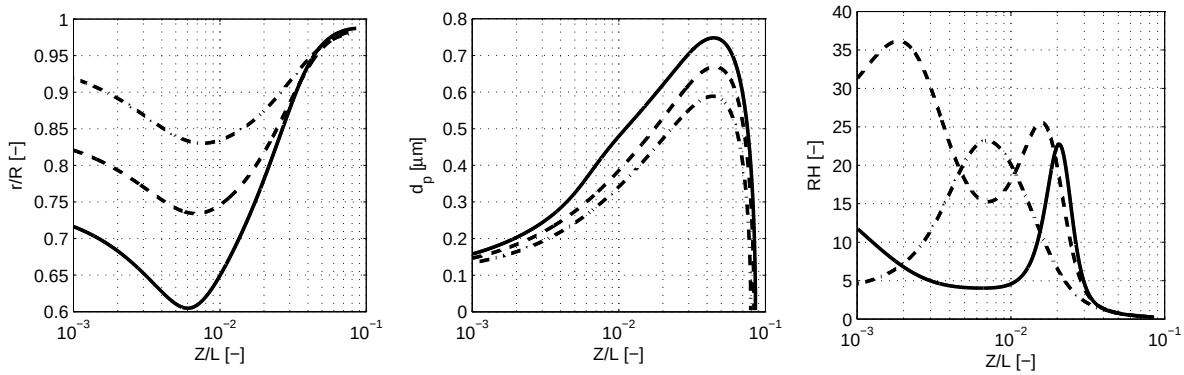

(a) (b) (c)

Figure 8: Result for a 0.1μm initial diameter droplet and $RH_{in} = 0.5$.(a) Dimensionless droplet position (droplets move from left to right), (b) droplet diameter and (c) relative humidity at droplet position. All are plotted as functions of the dimensionless axial coordinate. The different lines denote droplets released from different radial positions.

Comparing the cases for $d_{init} = 0.1\mu$m and $d_{init} = 0.5\mu$m with an inlet humidity of $RH_{in} = 0.5$ for both cases, shows that the droplet trajectories (figures 8a and 6a) are quite similar. It seems that the initial droplet size has only a slight influence on the trajectories. The inlet humidity does have a large influence on the domain in which droplets are found. Increasing the humidity leads to longer droplet trajectories and larger droplets which eventually are able to hit the wall.

To give an idea what the combined influences are, the simulation is repeated for a variety of droplets with a mean droplet diameter of 0.5μm and a standard deviation of 0.2μm. The droplets are released from $r_0/R = 0$ till $r_0/R = 1$ with 200 steps in between in order to obtain the liquid concentration. The computational domain is divided into cells in which the mass

weighted liquid concentration is calculated according to

$$C_{i,j} = \sum_{n=1}^{N} \frac{d_n^3}{r_n} \tag{8}$$

where n is the droplet number index, N the total number of droplets found in a cell with index (i, j) and r is the radial droplet position. The concentration is normalized with the maximum found in the case that $RH_{in} = 0$. The result is shown in figure 9 for inlet humidities $RH_{in} = 0$ and $RH_{in} = 0.5$.

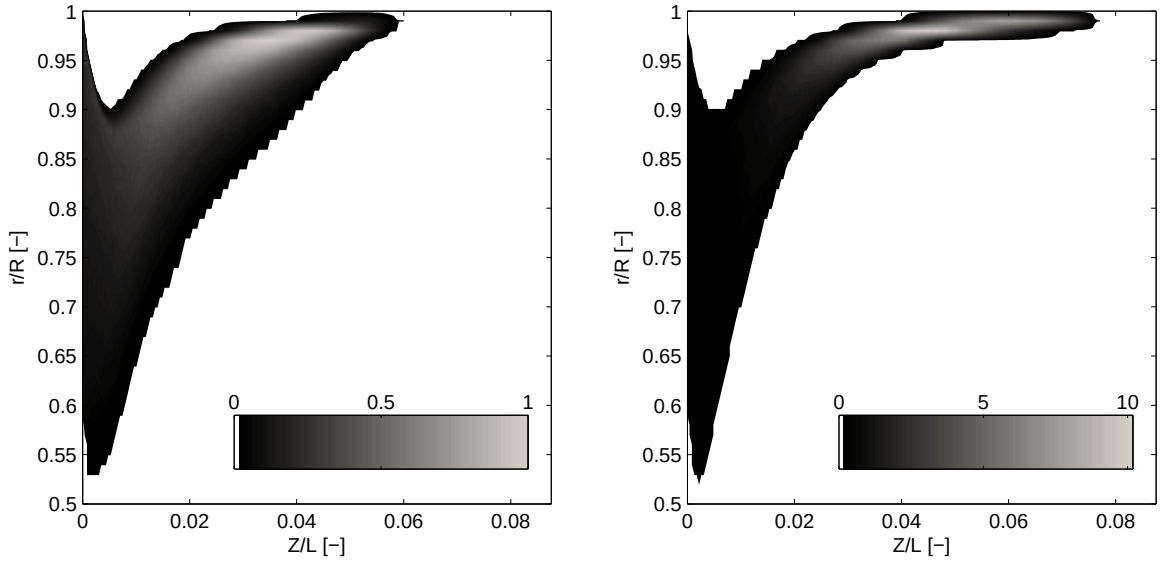

(a) (b)

Figure 9: Normalized liquid concentration for water droplets in the vortex tube. (a) $RH_{in} = 0$ and (b) $RH_{in} = 0.5$. Mind that the range of the grey scale for (b) is 10 times higher than (a)

The temperature in some regions of the vortex tube drops below the saturation temperature and the vapour becomes supersaturated. In this region condensation of vapour from the gas mixture onto the droplet occurs. The size of droplets and the liquid concentration therefore increase. When the temperature of the gas is above the saturation temperature, the opposite occurs: evaporation of droplets causes the liquid concentration to decrease towards zero.

Figure 9 shows that the maximum liquid concentration is found in the case where $RH_{in} = 0.5$ (figure 9b), and is more than 10 times higher than in the zero humidity case, shown in figure 9a. The figure makes also clear that the domain in which droplets are found (non-white regions) decreases for increasing humidity. Also the highest liquid concentration is found closer to the wall. The higher the liquid concentration near the wall, the more efficient the separation process is. It is therefore expected that adding additional contaminant in the gas (in this case water vapour), enhances the separation efficiency.

5. Conclusion

A MATLAB model is written in order to simulate droplet behaviour in the vortex tube. Results show the influence of humidity on droplet tracks and liquid concentration. The maximum liquid concentration is tremendously affected by the humidity. A more than 10 times higher liquid concentration is established if the nitrogen gas entering the vortex tube is humidified at $RH_{in} = 0.5$. Results show that increasing the humidity at the inlet of the vortex tube results in larger droplets and a higher liquid concentration and that the separation process should take place in the first few centimeters of the vortex tube. It is expected that this enhances the separation efficiency of the vortex tube as droplet separator.

Acknowledgments

This research is supported by the Dutch Technology Foundation STW, which is the applied science division of NWO, and the Technology Programme of the Ministry of Economic Affairs.

References

Bird, R. Byron, Stewart, W. E. & Lightfoot, E. N. 2007 *Transport Phenomena*. John Wilye & Sons, Inc.

Gao, C. 2005 Experimental study on the ranque-hilsch vortex tube. PhD thesis, Technical University of Eindhoven, the Netherlands.

Hilsch, R. 1947 The use of expansion of gasses in a centrifugal field as cooling process. *The review of scientific instruments* **18** (2), 108–113.

Janna, W. S. 2000 *Engineering Heat Transfer* 2^{nd} *Edition*. CRC Press.

Ranque, M. G. 1933 Experiences sur la detente avec production simultanees d'un echappement d'air chaud et echappement d'air froid. *J. de Physique et de Radium* **7** (4), 108–113.

Sazhin, S. S. 2005 Modelling of heating, evaporation and ignition of fuel droplets: combined analytical, asymptotic and numerical analysis. *Journal of Physics: Conf. Series* **22**, 174–193.

Sazhin, S. S., Abdelghaffar, W. A., Krutitskii, P. A., Sazhina, E. M. & Heikal, M. R. 2005 New approaches to numerical modelling of droplet transient heating and evaporation. *Int. Journal of Heat and Mass Transfer* **48**, 4215–4228.

Spalding, D. B. 1979 *Combustion and mass transfer*. Pergamon Press.